

MODIFIED CAPACITOR ASSISTED EXTENDED BOOST QUASI Z-SOURCE INVERTER FOR THE GRID-CONNECTED PV SYSTEM

HEMALATHA NAGAIYASAMY^{*} AND SEYEZHAI RAMALINGAM

*Department of Electrical and Electronics Engineering,
SSN College of Engineering, Chennai, India.*

^{}Corresponding author: rnhemaa@gmail.com*

(Received: 13th Dec 2018; Accepted: 1st March 2019; Published on-line: 1st June 2019)

<https://doi.org/10.31436/iiumej.v20i1.1042>

ABSTRACT: A grid-tied, single stage, three phase, PV system provides higher efficiency than a two-stage PV system. This paper presents a three-phase, single stage, grid-connected PV system with MPPT and reactive power injection capability into the grid using modified capacitor assisted extended boost quasi Z-source inverter (MCAEB q-ZSI) as the grid-tied PV inverter. The adaptability of the inverter for irradiance changes and the boost factor control with its shoot-through duty ratio adjustment made it highly recommended for the grid system. The shoot-through control technique like maximum constant boost control with a third harmonic injection enhances the performance of the inverter by reducing the low order ripples and voltage stress. The fuzzy voltage controller is proposed with the capacitor linearization algorithm to regulate the DC-link voltage. The current approach uses a fuzzy controller to control the real and the reactive power injection into the grid. The performance evaluation of the fuzzy and PI grid controller is carried out for the constant irradiance condition and from the investigation, parameters like boost factor (B), the shoot-through duty ratio(D_s), real power (P), reactive power (Q), power factor and harmonics in the current injection are determined. A laboratory setup of the PV powered grid system is implemented, tested and validated with the simulation results.

ABSTRAK: Dalam sistem fotovoltaik (PV) yang bersambung dengan satu peringkat, satu sistem elektronik kuasa yang mempunyai keuntungan dan kecekapan yang tinggi diperlukan untuk menginterupsi dengan utiliti tersebut. Dalam makalah ini, kapasitor yang diubah suai dibantu oleh pemacu kuadratik Z-source yang dilanjutkan (MCAEB q-ZSI) bertindak sebagai unit interfacing antara PV dan grid. Penyesuaian penyongsang untuk perubahan sinaran dan kawalan faktor rangsangan dengan pelarasian nisbah tugas menembak membuatnya sangat disyorkan untuk sistem grid. Teknik kawalan menembak seperti kawalan rangsangan berterusan maksimum dengan suntikan harmonik ketiga meningkatkan prestasi penyongsang dengan mengurangkan aruhan pesanan rendah dan tekanan voltan. Pendekatan semasa menggunakan pengawal kabur untuk mengawal suntikan kuasa sebenar dan reaktif ke grid. Penilaian prestasi pengawal grid fuzzy dan PI dilakukan untuk keadaan iradiasi malar dan dari penyiasatan, parameter seperti faktor rangsangan (B), nisbah tugas menembak (D_s), kuasa nyata (P), kuasa reaktif (Q), faktor kuasa dan harmonik dalam suntikan semasa ditentukan.

KEYWORDS: MCAEB q-ZSI; shoot-through; boost factor; MPPT; synchronization

1. INTRODUCTION

In photovoltaic applications, the nonlinearity of PV array characteristics due to varying environmental conditions like PV module operating temperature, irradiation, and partial shading effects produces a DC voltage that is intermittent in nature. This intermittent PV DC voltage, when fed to the AC side of the inverter, affects the reliability and system efficiency and produces poor quality in the power supplied to the grid [1]. Under such operating conditions, the grid-tied PV inverter features non-minimum phase characteristics with its output voltage causing an overshoot and undershoot in the capacitor voltages [2]. Such characteristics result in a poor transient response with increased harmonics in the inverter output voltage. Thus the selection of grid-tied PV inverter, which is highly reliable under all operating conditions, is necessary to regulate the current injection for the grid system. The power conditioning unit (PCU) plays a vital role in PV power generation in interfacing the PV with the grid and to increase the power capability of the PV, the PCU with a high power conversion efficiency is required. The PCU for a dual stage conversion system requires an intermediate DC-DC converter for the boosting operation which results in an increase in the power conversion stages and the switching device count [3].

Single-stage power conversion technology is becoming popular nowadays as it reduces the intermediate conversion stages, cost, and space requirements [4]. When the single-staged conventional quasi Z-source inverter is operated to achieve a high gain, this results in an increase in the switching voltage stress and a reduction in the efficiency due to the high power losses occurring in the conducting switching devices [5]. When such a type of inverter is acting as a power conditioner between the PV and the grid, it requires a number of PV panels to achieve a required voltage gain and the efficiency of the overall system gets reduced. Thus, an enhanced type of single-staged quasi inverter namely, the extended boost quasi Z-source inverter (EB q-ZSI), is evolved for improving the gain and designed using the same number of inverter MOSFET switches with reduced component ratings in the cascaded quasi impedance network [6,7]. Among the families of EB q-ZSI, capacitor assisted and diode assisted topology, the structural modification in the impedance network of modified capacitor assisted (MCAEB q-ZSI) provides high voltage gain with reduced voltage stress [8]. The cascaded impedance network includes the passive components for its design and it aids in the boosting operation by the shoot-through duty cycle adjustment.

The maximum constant boost control with the third harmonic injection method is the most suited PWM technique for an MCAEB quasi inverter, as the technique does not give rise to low-frequency ripples in the inductor current and capacitor voltage waveform [9]. The total elimination of the low order triplen harmonics from the output voltage totally reduces the harmonic content in the output and the filtering component ratings. The current harmonics in the output current is less than 5% and the total harmonic distortion (THD) in the output of the proposed inverter is within the permissible range of IEEE 1547 grid standards. The maximum utilisation of the zero states by the shoot-through pulse brings down the voltage stress across the switching device [10]. Thus this technique provides an excellent output voltage controllability with increased gain and boost factors. The most desirable features of MCAEB q-ZSI, make it function as a grid-tie PV inverter for the grid-connected PV system. This inverter drives the PV array to operate at the maximum power point (MPP) under the time-varying irradiance and module operating temperature conditions. This generates an AC output voltage in phase with the grid voltage, balances properly the average power delivered to the grid and provides a quality of power to the utility by its grid integration [11].

The closed-loop control of the grid PV system is realized by grid synchronization, MPPT control, DC link voltage control and the current control approach. The proper design of the grid controller suppresses the effects of current harmonics to provide a proper power flow of active and reactive power into the grid [12]. The fuzzy logic based grid controller is proposed to provide a proper feedback control of the shoot-through duty ratio to normalize the DC link capacitor voltage, to maintain the grid current injection to be sinusoidal, and to achieve a high dynamic performance with THD less than 5%. The grid controller with a dual loop control algorithm has the inner current and the outer voltage control loop [13]. The DC-link voltage controller, in spite of the input disturbances due to the changes in the irradiation level, regulates DC-link voltage (V_{dc}) by adjusting the shoot-through duty cycle of the inverter [14]. It prevents the PV array side disturbances to be passed to the inverter AC side, thereby helping in the extraction of the maximum extent of the PV power. The current controller limits the current harmonics and controls the proper power flow into the grid by affording a good output voltage regulation. The performance evaluation between proportional-integral and fuzzy logic grid controller reveals that the response of the fuzzy voltage controller to the input side disturbances is faster by providing a good input voltage regulation than the PI controller. To the load disturbances, the fuzzy current controller responds quicker, thereby providing an excellent power management control. Thus, the closed-loop control of the grid PV system with fuzzy MPPT and grid controller was proposed and tested for constant irradiation and the prototype was developed to validate the test conditions.

2. PROPOSED MCAEB q-ZSI FED GRID TIED PV SYSTEM

The representation of the PV system with the various controllers are shown in Fig. 1. The presented system has a PV array, MCAEB quasi-inverter, LCL filter, coupling transformer, utility and a lamp load for testing. The controllers involved are the fuzzy MPPT controller, PWM controller, and fuzzy based grid controller. A 500W PV powered grid system is considered for testing and the system is simulated in MATLAB for a uniform irradiation condition and the system specifications presented in Table 1.

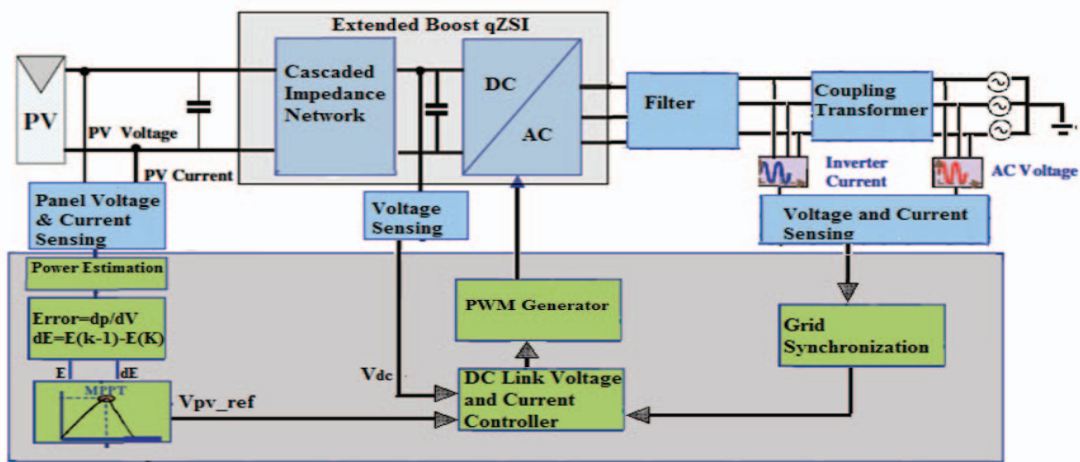


Fig. 1: Block diagram of PV powered MCAEB q-ZSI fed grid system.

2.1 PV Array

The PV array forms the input DC source and the available DC power from the array decides the grid injected real power (P). A PV model is developed by a step-step

procedure in MATLAB and is tested for a constant irradiance of 1000 W/m^2 . The PV array voltage and current at maximum power point (MPP) are presented in Figs. 2 and 3.

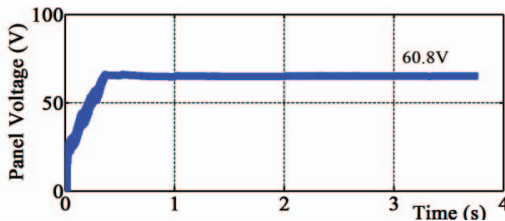


Fig. 2: PV array voltage at constant irradiance.

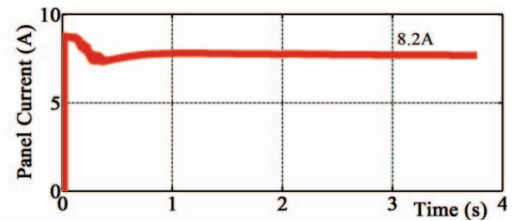


Fig. 3: PV array current.

After testing the developed PV model, it is observed that the PV array voltage at the maximum power point (MPP) settles at 60.8 V and the PV current at 8.2 A. Now the tested model is directly interfaced with the grid using the three-phase modified capacitor assisted extended boost quasi Z-source inverter (MCAEB q-ZSI) as the power conditioner.

Table 1: System specification

Solar Array Specification		Inverter Specification	
Parameters	Ratings	Parameters	Ratings
Output Power (P_{\max})	500 W	KVA rating	500 VA
PV output voltage	73 V	Output AC voltage	220V $V_{ac(P-P)}$
PV current	8.8 A	No. of Phases	3ø
V_{MPP} & I_{MPP}	61 V, 8.2 A	Inverter Frequency	50 Hz
Cells per module	72	Switching Frequency(f_s)	8 KHz
Coupling Transformer Specification		Filter & Grid Specification	
Parameters	Ratings	Parameters	Ratings
No. of Phases	3ø	Filter inductance	$720 \mu\text{F}$
Primary voltage rating	110 V	Filter capacitance	2.4 mH
Secondary voltage rating	230 V	Grid voltage	415 V, AC
Primary current rating	4.56 A	Grid frequency	50 Hz
Secondary current rating	1.2 A	No of Phases	3ø
Connections	$\Delta-\lambda$		

2.2 Modified Capacitor Assisted Extended Boost Quasi ZSI (MCAEB q-ZSI)

In this proposed system, MCAEB q-ZSI is deployed as the grid-tied inverter for interfacing the PV array with the grid and in a single stage process, the energy conversion from DC-AC takes place with a high gain. The circuit diagram of the proposed inverter is depicted in Fig. 4. The modified topology of the CAEB q-ZSI decreases the operating voltages of the capacitors in the impedance network and reduces the device ratings. The circuit operates in active mode and the shoot-through state for the power transfer from the source to the load. The cascaded quasi-impedance network is designed using the capacitors, diodes and inductors that aid in the boosting of the PV voltage to the voltage level required during the shoot-through operation [15]. The maximum constant boost control (MCBC) with a third harmonic injection PWM method is proposed for this inverter and this technique suppresses the lower order triplen harmonics, thereby reducing the switching stress with a reduced filter component size [16]. The inverter is operated with the

modulation index (m_a) set to 0.9908 and D_s to 0.1418 in order to achieve a boost factor of 1.7416 for the constant solar irradiation. The different waveforms of MCAEB q-ZSI before filtering is portrayed in Fig. 4. The waveform for the boost voltage is represented in Fig. 5(a) and the waveform for the inverter output line-line voltage before filtering is displayed in Fig. 5(b). The waveforms for the phase voltage and the inverter phase current are represented in Fig. 5(c) and 5(d).

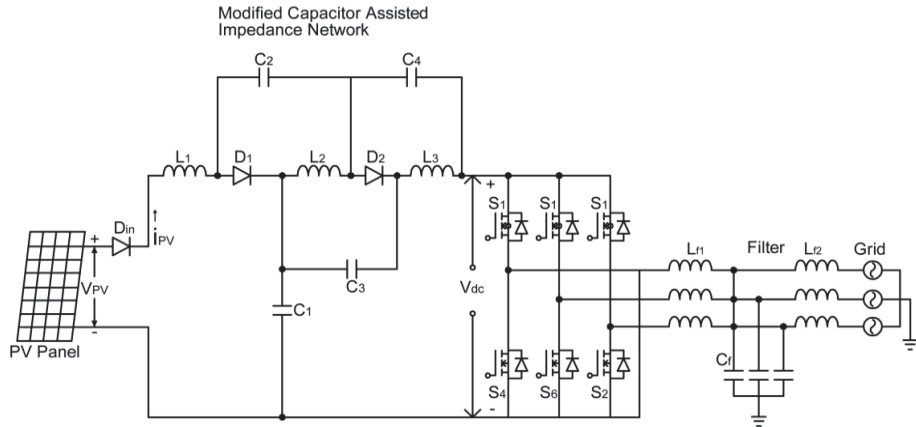


Fig. 4: Circuit diagram of MCAEB q-ZSI fed PV system.

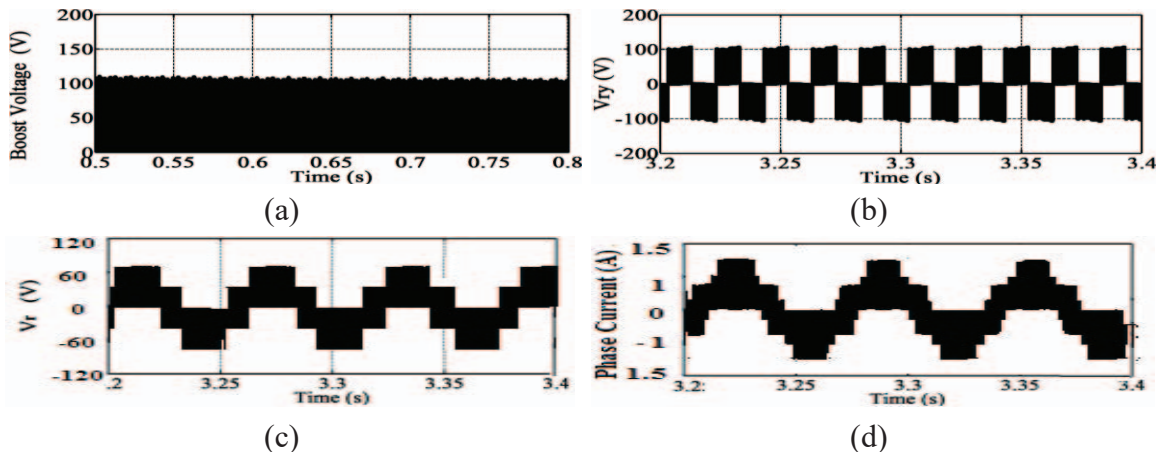


Fig. 5: Waveforms of MCAEB q-ZSI before filtering (a) DC link voltage (b) inverter output line-line voltage before filtering (c) output phase voltage (e) output phase current.

Figure 5(a) infers that the DC link voltage (V_{dc}) obtained from the boost operation of the inverter is 110 V showing that the required boost factor is obtained and Fig. 5(b) shows that the AC line-line voltage (V_{P-P}) is 22 V before filtering. Figure 5(c) and 5(d) represent that the phase voltage and current are 64.2 V and 1.46 A, respectively. The voltage gain provided by the proposed inverter during this operation is 1.7956 and it is most suitable for grid integration.

2.3 LCL Filter

The shunt-type LCL filter is most commonly used nowadays as it provides high filtering characteristics with its low-cost design to attenuate the harmonics. The inverter voltage output is passed to the LCL filter with the filter capacitance values C_1 , C_2 and C_3 to be $720\mu F$ and the filter inductance values $L1$ and $L2$ to be 2.4 mH . The three-phase line

voltages and currents after filtering are shown in Fig. 6(a) and 6(b). The voltage and current THD are presented in Fig. 6(c) and 6(d).

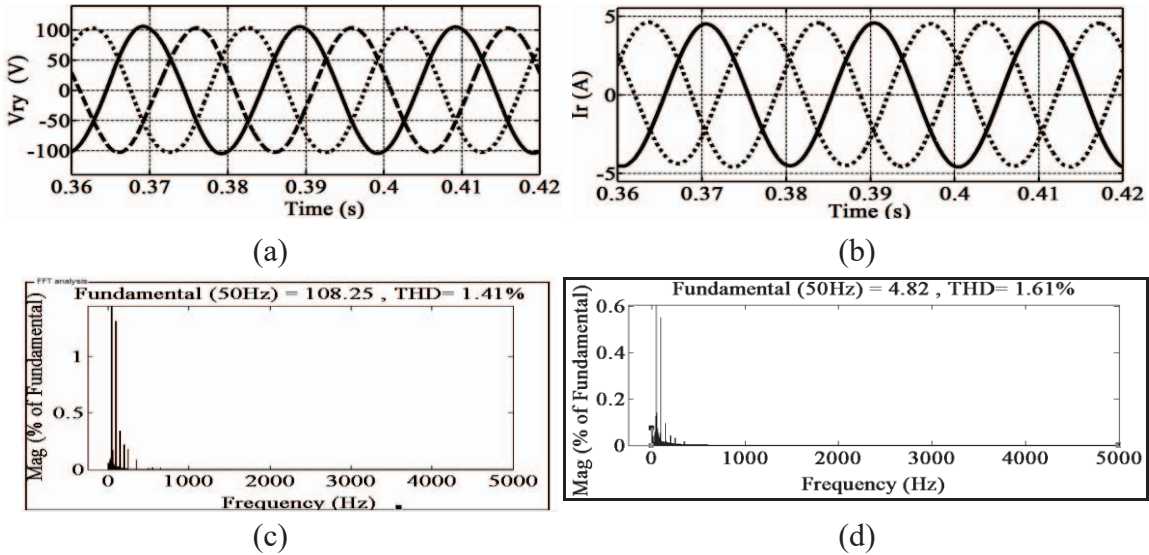


Fig. 6: Waveforms of MCAEB q-ZSI after filtering (a) output line-line voltage (b) output line-line current (c) THD in filtered output voltage (d) THD in the filtered output current.

The filtered peak-peak line voltage is 220 V and the peak inverter current is 4.82 A. The proposed LCL filter reduces the current harmonics provided by the grid-tied inverters and is limited to 1.61%, which meets the grid standards for the current injection.

2.4 Coupling Transformer

A step up coupling transformer provides a galvanic isolation link between the PV and the grid. This separation reduces the dangerous operations on the PV side caused by a fault occurring on the grid side. The inverter voltage is stepped to the value to match the grid voltage and the output waveforms are represented in Fig. 7.

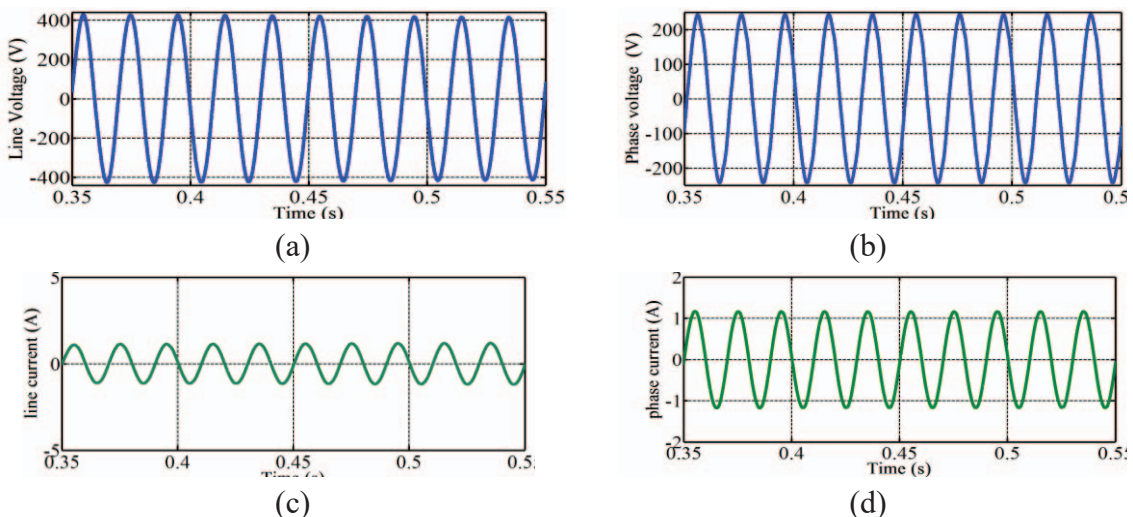


Fig. 7: Waveforms of the transformer (a) output line voltage (b) output phase voltage (c) output line current (d) output phase current.

Figure 7 infers that the output of the coupling transformer is stepped to the voltage level of 415 V and the per phase voltage is 230 V. The output phase current is 1.2 A and the output line current is 1.2 A as the transformer is in Delta-Star connection.

3. CONTROL SCHEMES FOR MCAEB Q-ZSI FED GRID-CONNECTED PV SYSTEM

The inverter control schemes such as grid synchronization, MPPT control algorithm, DC-link voltage control and the power management control with the current control are operated together to perform the closed loop control operation of the proposed grid system. The schematic diagram of the grid-tied PV system is presented in Fig. 8. The fuzzy based grid controller with a modified voltage controller using the linearized capacitor voltage control is proposed and the fuzzy current controller is utilized for power management control.

3.1 Grid Synchronization

In a PV grid system, the grid synchronization is to be considered in which the phase angle, voltage magnitude, and frequency of grid-tied inverter must match with that of the grid standards. The phase angle and the grid frequency estimated by the three-phase phase-locked (PLL) loop provides the proper operation of the inverter control algorithm. The PLL technique based on the synchronous reference (SRF) frame method determines the grid phase angle (θ) accurately and the structure of the PLL to perform this work is portrayed in Fig. 9(a).

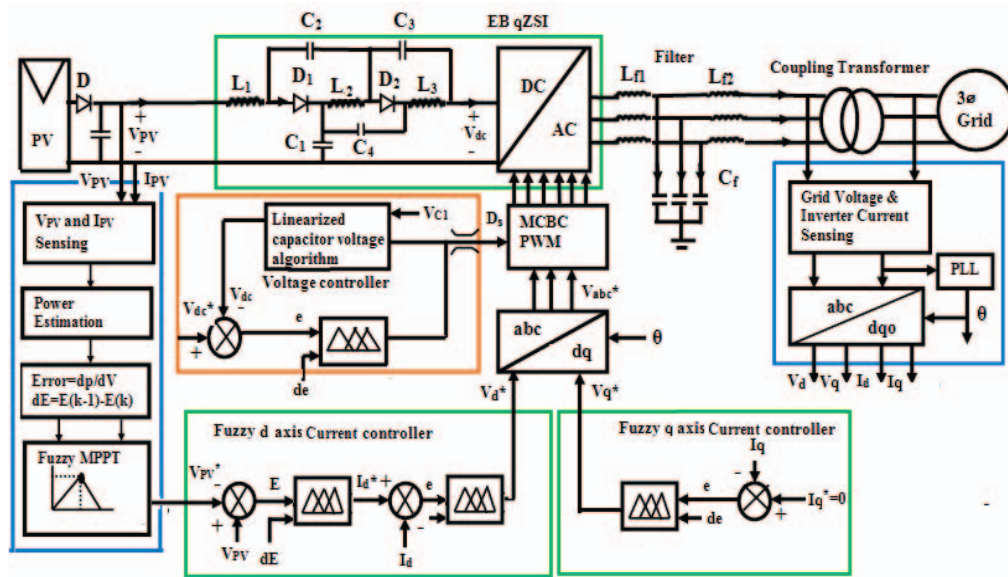


Fig. 8: Schematic diagram of a PV powered grid-tie system.

In the d-qo transformation block represented in Fig. 9(a), the three-phase grid voltages (V_{abc_grid}) and the inverter current (I_{abc_inv}) are transformed into d-q axis quantities. The inverter currents (I_{abc_inv}) and grid voltages (V_{abc_grid}) are filtered out and are passed to the d-qo transformation block for transferring into d-qo quantities. The transformed d-qo quantities such as V_d V_q and I_d I_q are portrayed in Fig. 9(c) and 9(d). The estimated PLL phase angle (θ) and the grid frequency identified are displayed in Fig. 9(e) and 9(f). The grid phase angle (θ) is estimated for the normal grid conditions and the estimated grid frequency is found to be 50 Hz, which closely matches the grid standards provided in

IEEE 1547 standards. The synchronization of the inverter current and the grid voltage is portrayed in Fig. 10(a). The grid phase angle in locking mode with the grid reference signal is given in Fig. 10 (b).

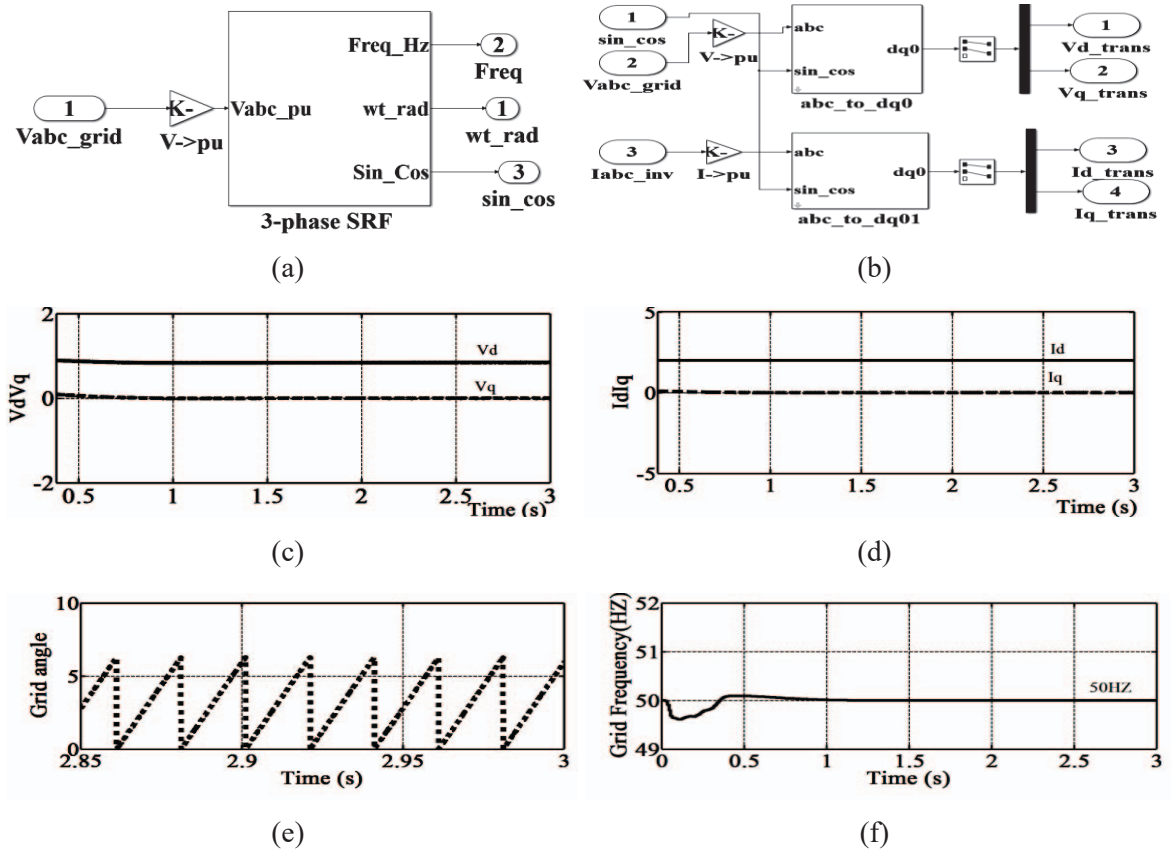


Fig. 9: (a) SRF based PLL (b) adc-dqo transformation block (c) transformed V_dV_q (d)transformed I_dI_q component (e) grid phase angle (f) grid frequency.

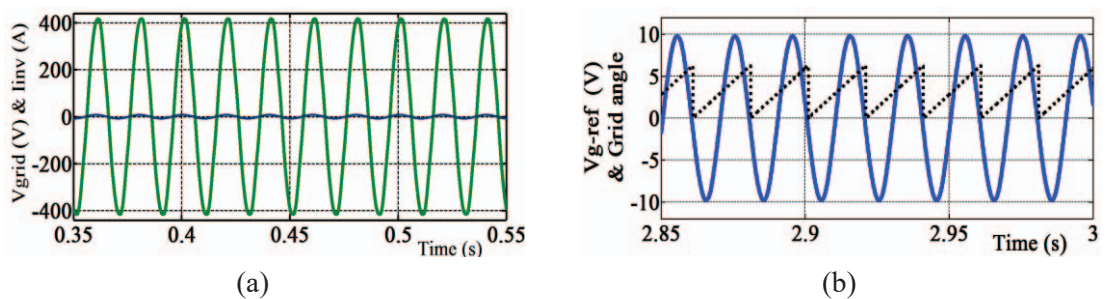


Fig. 10: (a) Grid Synchronization of grid voltage and the inverter current, (b) Locking mode of the grid reference signal and grid phase angle.

Under the normal operating conditions of the grid, grid voltage and the inverter current are found to be in synchronism in the grid mode. In this mode, the grid angle and the grid reference signal are in synchronism for a normal steady grid. When the abnormal grid conditions occur, the inverter should work in an anti-islanding mode and suddenly withdraw the PV system from the grid.

3.2 MPPT Control

In this proposed PV system, the fuzzy MPPT tracker is incorporated with it for the maximum PV power extraction and is presented in Fig. 11. The fuzzy MPPT tracker performs its tracking operation in uniform and varying irradiance conditions and provides excellent results without fluctuations while tracking the MPP in this proposed system[18].

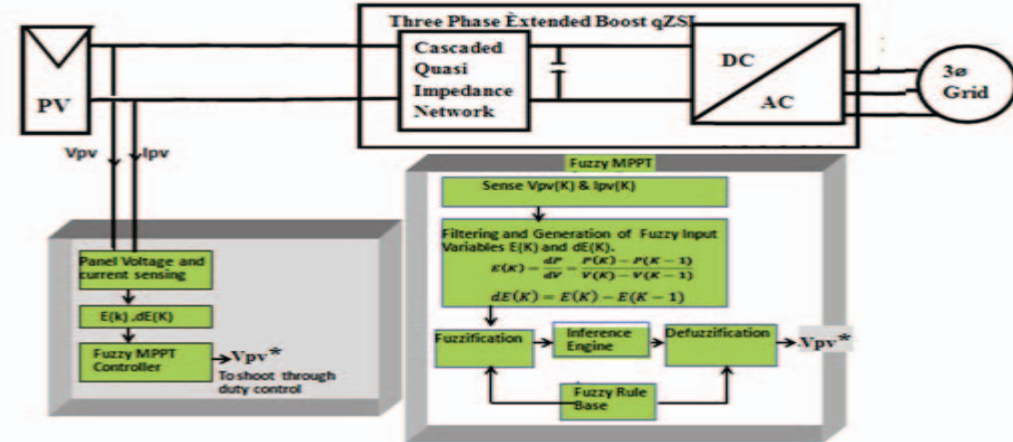


Fig. 11: Fuzzy MPPT Control.

Under the uniform irradiation conditions of 1000 W/m^2 , the MPPT tracker tracks the maximum power point (MPP) in the proper direction without losing its control by getting input information about the error and change in the error signal. The MPPT reference voltage (V_{PV}^*) at which the maximum power occurs is located at the knee of the characteristic curve. Figure 12 presents the PV characteristics representing the array power, voltage and current at MPP.

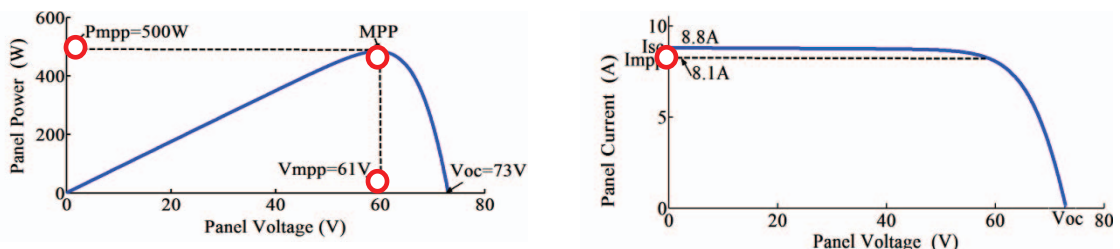


Fig. 12: (a) Array power vs voltage, (b) Array voltage vs current.

The reference voltage V_{PV}^* from the controller under such uniform irradiance condition is 60.8 V and this, in turn, is applied to the voltage controller for tuning D_s in the PWM controller. D_s is controlled to 0.1414 so that B of the inverter is maintained at 1.7416 and the voltage across the capacitors is maintained at 110 V. Thus the fuzzy MPPT control performs efficiently providing a good response with less ripple at MPP.

3.3 Grid-Connected Inverter Control

The fuzzy logic grid controller with the DC link voltage and the current controller is proposed for this PV system [19,20]. The voltage controller controls the DC link voltage (V_{dc}) to manage the power flow into the utility. The current controller has the capability to control the current injection into the grid and is responsible for the power quality issues.

3.3.1 DC Link Voltage Controller

In this controller, a linearized capacitor voltage control algorithm used in maintaining DC-link voltage is proposed. The capacitor voltages from the cascaded q-ZS network and the input PV voltage (V_{PV}) are used to estimate the duty ratio (D_s), which in turn controls the boost factor (B) of the inverter and DC link voltage (V_{dc}).

$$V_{dc} = V_{C1} + V_{C2} + V_{C3} \quad (1)$$

$$V_{C1} + V_{C2} + V_{C3} = V_{PV} * \left(\frac{1}{1 - 3D_s} \right) \quad (2)$$

$$\frac{V_{C1} + V_{C2} + V_{C3}}{V_{PV} * \frac{1}{1 - 3 \cdot \frac{T_S}{T}}} = \frac{1}{1 - 3 \cdot \frac{T_S}{T}} \quad (3)$$

Eq. (2) shows that the relationship between the capacitor voltages and D_s are non-linear. This non-linearity in the capacitor voltages is due to the fluctuating nature of the PV, thereby resulting in an increase in the voltage ripple in the DC link voltage waveform. This is overcome by the linearized capacitor voltage control algorithm.

$$\frac{T_S}{T} = \frac{1}{3} \left[1 - \frac{1}{\left(\frac{V_{C1} + V_{C2} + V_{C3}}{V_{PV}*} \right)} \right] \quad (4)$$

$$\frac{T_S}{T} = \frac{1}{3} \left[1 - \frac{1}{K} \right] \quad (5)$$

$$D_s = \frac{1}{3} \left[\frac{K - 1}{K} \right] \quad (6)$$

where $K = \frac{V_{C1} + V_{C2} + V_{C3}}{V_{PV}*}$. The fuzzy based DC link voltage controller with the capacitor voltage linearization algorithm is presented in Fig. 13. V_{C1} , V_{C2} & V_{C3} are measured and the sum of these voltages (V_C) determines DC-link voltage (V_{dc}). The MPPT reference voltage V_{PV}^* is obtained from the fuzzy MPPT controller and $V_{ip} = \frac{V_C}{V_{PV}*}$ is determined from it. The reference voltage V_{ip}^* is set and is compared with V_{ip} to generate the error signal (E). The change in the error signal (dE) and the error signal (E) are given as inputs to the fuzzy voltage controller. The output signal from the controller is given to limiter and the value of constant K is obtained. This is fed to the D_s calculation block to obtain D_{s_ref} . The controller is quick in response to the reference voltage generated from the MPPT controller and accordingly, K and D_s are adjusted. The constant K controls the capacitor voltages in the impedance network and the range of K is $1 < K < \frac{V_C}{V_{PV}*}$. Thus the capacitor voltages are regulated and the DC-link capacitor voltage is maintained to the required boost level. The subsystem for the fuzzy voltage controller is displayed in Fig. 14.

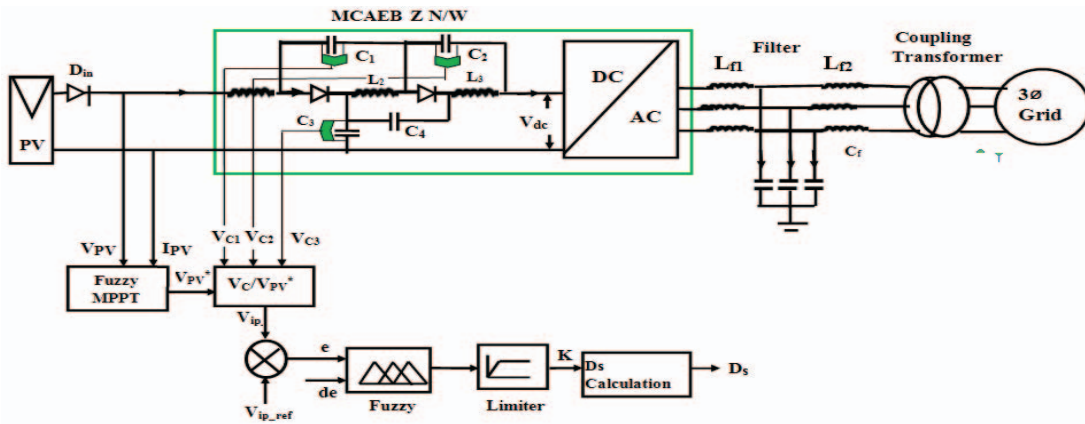


Fig. 13: Proposed Fuzzy based DC link voltage controller.

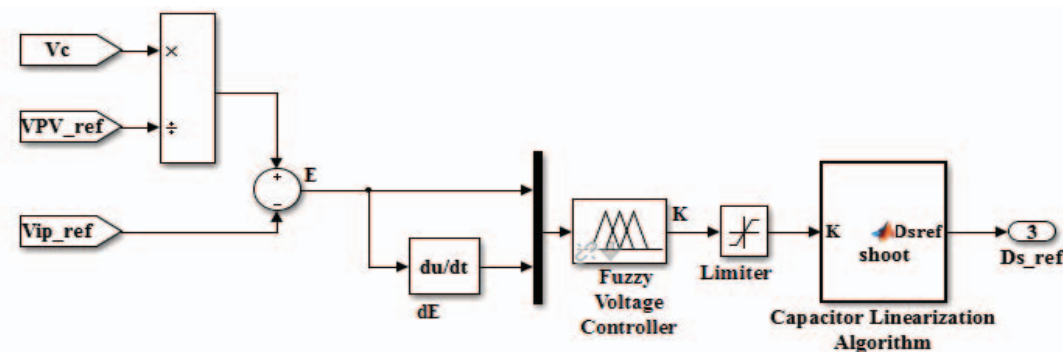


Fig. 14: The subsystem of the fuzzy voltage controller.

The controller responds quickly in adjusting its control signal K value for the applied uniform irradiance level. The time response of fuzzy and the PI voltage controller in reaching the steady-state of the DC-link capacitor voltage is portrayed in Fig. 15. The performance evaluation of fuzzy with the PI controller is tabulated in Table 2.

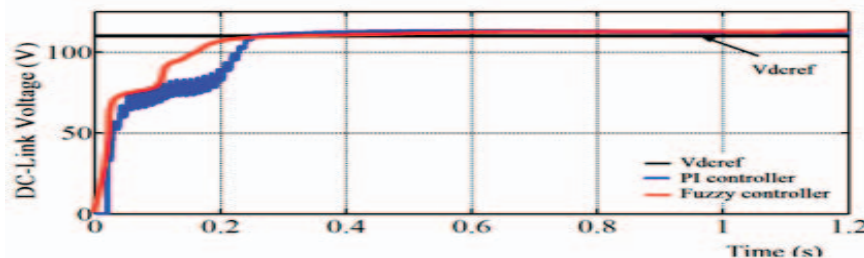


Fig. 15: Response of the fuzzy and PI voltage controller.

Table 2: Comparison of fuzzy and PI voltage controller

Irradiance Level [W/m ²]	V _{MPP} [V]	D _s _ref	Settling Time of PI controller, [s]	Settling Time of fuzzy controller, [s]
000	61.2	0.1414	0.28	0.2

For this irradiation level, MPPT reference voltage V_{PV}^* obtained from MPPT controller is 61.2V, the voltage controller tunes the control signal K value to 1.809. D_s value is adjusted to 0.1414 so that V_{dc} is maintained at 110V. The time response of the proposed controller in reaching the steady DC-link voltage is 0.2s, whereas PI controller

settles at 0.28s. From Table 2, it is inferred that the response of the proposed voltage controller is excellent and it responds faster to the changes in the MPPT reference voltage than the PI controller.

3.3.2 AC Side Current Controller

The grid current controller is used to supply a current injection into the grid with a reduced current harmonics and for managing a steady power flow into the utility grid in spite of input and load disturbances. The grid voltage varies with the instant of time and the current reference (I_{dref}) has to be adjusted in accordance with the grid operating conditions so as to maintain a required active and reactive power feeding into the utility. By Park's transformation, the grid voltage is converted to DC quantities for analysis purposes. The real (P) and reactive (Q) powers are controlled by the current control approach of the grid-connected inverter control algorithm by controlling the direct axis (d) and quadrature (q) axis currents separately. The fuzzy current controller has d-axis and q-axis controllers that are the active and the reactive power controllers are portrayed in Fig. 16. The power equations in DQ form are given as follows.

$$\text{Real power } P = \frac{3}{2}(V_d I_d + V_q I_q) \quad (7)$$

$$\text{Reactive power } Q = \frac{3}{2}(V_q I_d - V_d I_q) \quad (8)$$

When the synchronous reference frame is aligned with the grid voltage, the quadrature axis component $V_q = 0$ and the power equations are reduced as follows.

$$P = \frac{3}{2}(V_d I_d) \quad , \quad Q = -\frac{3}{2}(V_d I_q) \quad (9)$$

Eq. (9) and Eq. (10) infers that, the real and reactive powers are controlled independently by controlling the dq current components (I_d and I_q).

$$\text{d axis current reference } I_d^* = \frac{2}{3} \left(\frac{P}{V_d} \right) \quad (10)$$

$$\text{q axis current reference } I_q^* = -\frac{2}{3} \left(\frac{Q}{V_d} \right) \quad (11)$$

The product of the reference voltage V_{PV}^* from the MPPT and I_{PV} , the function of V_{PV}^* are processed in N/D block to generate d axis current reference (I_d^*). I_d^* is compared with the measured value of the direct axis current component(I_d) and the error signal (e) is generated. E and dE signals are processed in the d-axis current controller and the output signal is the direct axis voltage reference (V_d^*). I_d^* controls the amount of current injection with respect to the reference voltage generated from MPPT control, thus regulating the real power flow. The q-axis current reference (I_q^*) is set to 0 and is compared with I_q to minimize the grid injected reactive power.

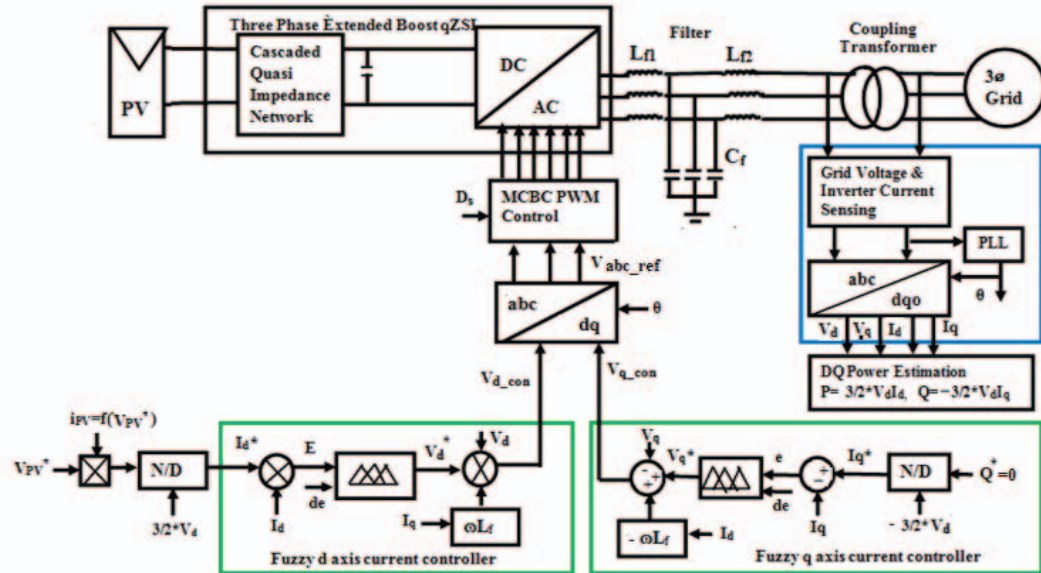
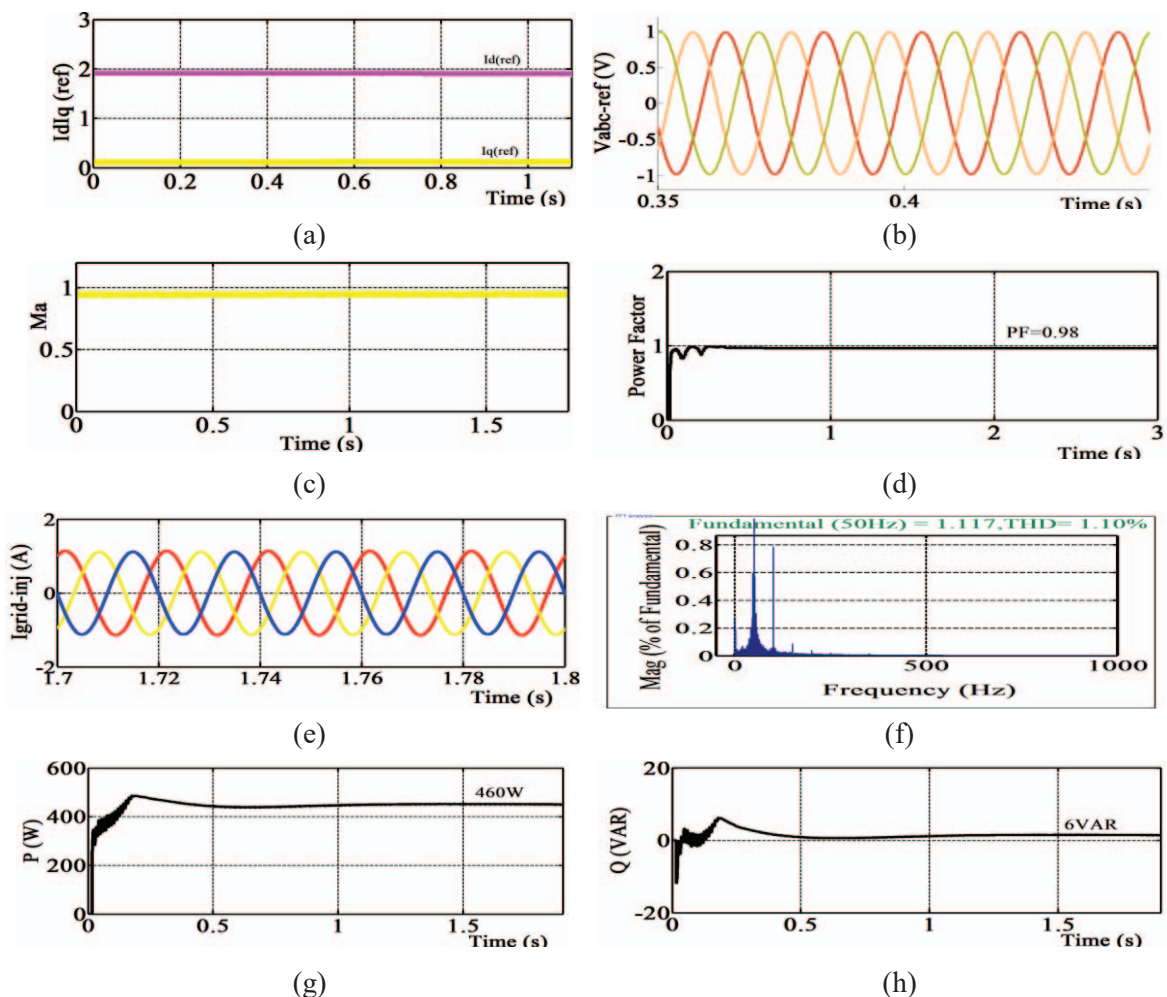


Fig. 16: Fuzzy current controller.

Fig. 17: Simulation results of fuzzy controller (a) $IdIq$ (ref) (b) modulating reference signals (c) ma (d) power factor (e) grid injected current (f) THD in grid injected current (g) real power (h) reactive power.

The input signals are processed in the q-axis controller and V_q^* is taken as the output from the controller. The reference modulating signals in d-q-o form is V_{d_con} and V_{q_con} and are transformed to V_{abc_conv} in the inverse d-q-o-abc transformation unit. The reference modulating signals in abc form (V_{abc_ref}) is generated, which controls the modulation index of the inverter. The reference modulating signals (V_{abc_ref}) and D_s_ref are given as inputs to the PWM controller with a maximum constant boost algorithm with the third harmonic injection technique for producing the firing pulses for the inverter switches. Thus the capacitor voltages, DC link voltage and the output voltage of the inverter are controlled for the constant irradiance condition, which in turn controls the injected grid current. The simulation is performed for a uniform irradiation level of 1000 W/m^2 and the simulation results waveforms are shown in Fig. 17.

The fuzzy current controller reacts to the reference voltage response signal from the MPPT controller. The reference d axis component (i_{dref}) is set to 1.9 and reference q axis component (i_{qref}) is 0.2. The modulation index settles at 0.9907 and power factor is 0.98 which is closely matches the grid norms. The generated real power from the proposed system is 460 W and 1.17 A is the current injection into the grid. The injected current is injected into the grid depends on the amount of PV generated reference voltage. The reactive power injected into the grid is 6VAR and it shows that the reactive power is minimized. Total harmonic distortion (THD) in the grid injected current is 1.10% and is within the permissible value of grid standards. The time response of fuzzy and PI current controller in reaching the steady-state real power is shown in Fig. 18. The performance comparison of the proposed current controller to that of PI controller is given in Table 3.

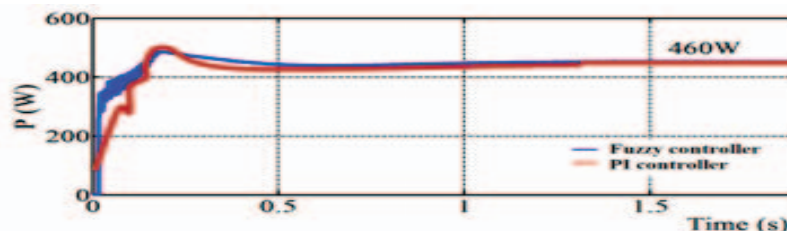


Fig. 18: The response of fuzzy and PI current controller.

Table 3: Comparison of fuzzy and PI current controller

Irradiance Level [W/m ²]	P [W]	m_a	Settling Time of PI controller, [s]	Settling Time of fuzzy controller, [s]
1000	460	0.9907	0.72	0.51

The settling time of the fuzzy controller in reaching the steady state value of the grid real power is 0.51s and in case of the PI controller, it is 0.72s. From Table 3, it is clear that shows that the response of the fuzzy controller is quicker than the PI controller.

4. EXPERIMENTAL RESULTS

A laboratory setup of MCAEB q-ZSI based grid PV system is developed and the snapshot of the prototype is presented in Fig. 19. The main power circuit consists of MCAEB q-ZSI with six IRF460N type MOSFET switches with the rating of 300V/30A. The switching device used for the proposed inverter is a fast switching N-channel enhancement mode MOSFET. The electrolytic capacitors ratings used in the q-ZS network

are $470 \mu\text{F}$ / 400 V, the ratings of toroidal inductors are 1mH and the Schottky diodes rating is 200 V / 20 A. The filter inductance is 1 mH and the filter capacitance is $2.2 \mu\text{F}$ / 450 V. The hall sensor XX054 is used for sensing the inverter output current. The three single-phase transformers of rating 24V-0-24V/5A are connected in delta-star connection to provide a necessary secondary side voltage rating of 230 V. The output from the coupling step-up transformer is given to the 100 W lamp load of each phase for testing.



Fig. 19: Photograph for the laboratory setup of MCAEB q-ZSI fed grid system.

The three-phase grid voltages undergo the signal conditioning operation using LM324 for manipulating the signal from 230 V to 6 V for the next stage of processing. The three-phase reference signal and the inverter output current from the hall sensor are given to the zero crossing detector circuit (ZCD) made with OPAMP LM358 for phase detection. The hardware prototype consists of MCAEB q-ZSI incorporated with the fuzzy MPPT tracker and is realized using the Pic18F45K22 controller. The AC side inverter control is programmed in the dsPIC3074011. The control signal from the fuzzy MPPT, the output signal from ZCD are given to the dsPIC30F4011 for inverter control and pulse generation. The generated pulses are fed through the gate drive circuit TLP250 to the gates of MOSFET switches with the switching frequency 7.66 KHz. The waveforms of the experimental results of the proposed system are portrayed in Fig. 20.

The input voltage, gate pulses and boost voltage are represented in Fig. 20(a), 20(b) and 20(c). The inverter output waveforms are displayed in Fig. 20 (d) - 20 (g). The grid synchronization of inverter current and the grid reference signal is presented in Fig. 20(h). The output voltage and current of the coupling transformer are presented in Fig. 20 (i) and Fig. 20(j). The hardware results show that the proposed topology produces a boost voltage of 109.4 V for an input DC voltage of 73 V. The boost factor provided by the inverter is 1.7635 and closely matches the simulated results of the boost factor. The peak-peak inverter AC line voltage is of 222.4V (V_{p-p}) and the peak-peak line current is 4.96 V. Figure 20 (f) shows that both the line currents I_r and I_y are phase shifted by 120° . Figure 20(h) infers that the grid reference signal after signal conditioning and the output inverter current from hall sensing are found to be in phase with each other, matching one of the main factors of grid synchronization. The inverter line voltage level is passed to the coupling transformer for stepping up the voltage level and the grid injected current is found to be 556mv. The lamp load connected across the transformer output consumes the power and starts glowing, indicating the current injected into the grid. Thus the experimental results are proven with the simulated results.

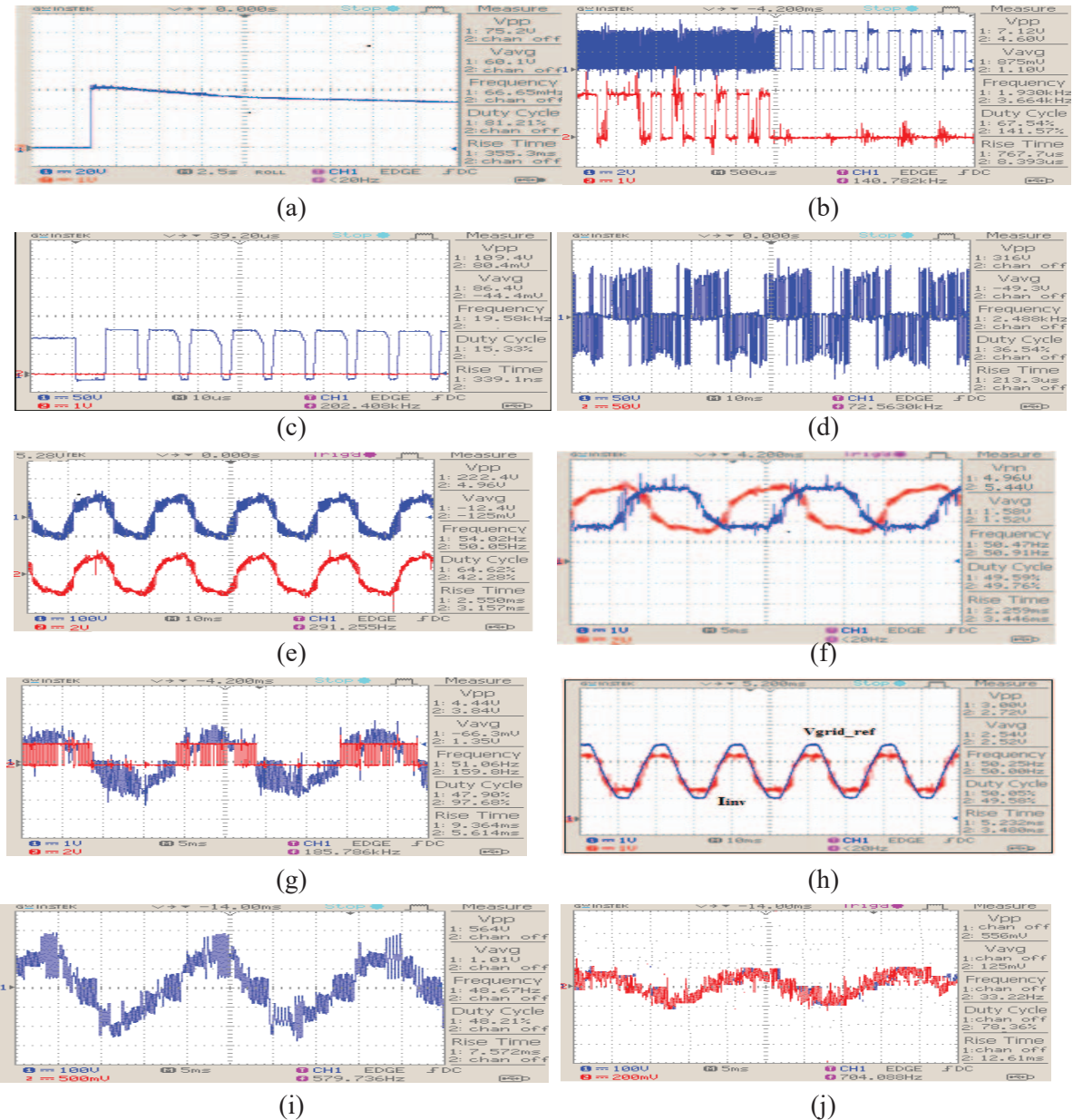


Fig. 20: (a) Input voltage (b) firing pulses (c) boost voltage (d) inverter voltage (e) filtered line voltage and current (f) filtered line currents (g) gate pulse (h) grid reference signal and inverter current (i) transformer output voltage (j) grid injected current.

5. CONCLUSION

In this paper, a single-stage MCAEB q-ZSI fed PV grid system is presented and discussed in detail with the closed loop operation of the system. The overall system has been simulated in MATLAB/Simulink with constant irradiance levels. Under such working conditions, the fuzzy voltage controller adjusts the shoot-through duty cycle of the gate pulses and regulates the boost factor so as to keep a constant DC link voltage. Thus the input side disturbance is not transmitted to the inverter AC side without affecting the grid current injection. The steady-state DC link voltage is attained by the fuzzy voltage controller at 0.2 s and the fuzzy MPPT provides a good tracking performance and it tracks the reference voltage at 0.54 s. The response of the current controller is excellent and the time taken for the steady state attainment of real power is 0.51 s. From the simulation, the

parameter investigation like the variations in the boost factor, D_s , real power, reactive power, the power factor and the harmonics in the current injection are determined and THD in the output voltage of the proposed inverter is found to be 1.104%. Finally, a hardware setup of a PV powered grid system with MCAEB q-ZSI acting as the grid-tied inverter is developed and implemented in the laboratory. The prototype model is tested for a uniform input condition and the tested results are validated with the simulated results.

ACKNOWLEDGEMENT

The authors wish to thank the management of SSN institutions for providing the computational facilities to carry out this work.

REFERENCES

- [1] Mastromauro RA, Liserre M, Dell'Aquila A. (2012). Control issues in single-stage photovoltaic systems: MPPT current and voltage control. *IEEE Transactions on Industrial Informatics*, 8(2):241-254.
- [2] Li Y, Jiang S, Cintron-Rivera JG, Peng FZ. (2013). Modeling and control of quasi-z-source inverter for distributed generation applications. *IEEE Transactions on Industrial Electronics*, 60(4):1532-1541.
- [3] Chen L, Amirahmadi A, Zhang Q, Kutkut N, Batarseh I. (2014). Design and Implementation of Three-Phase Two-Stage Grid-Connected Module Integrated Converter. *IEEE Transactions on Power Electronics*, 29(8) : 3881-3892.
- [4] Sher HA, Rizvi A, Addoweesh KE, Al-Haddad K. (2017). A Single-Stage Stand-Alone Photovoltaic Energy System With High Tracking Efficiency. *IEEE Transactions on Sustainable Energy*, 8(2):755-762.
- [5] Peng Shuangjian, An Luo, Yandong Chen, Zhipeng LV. (2011). Dual-Loop Power Control for Single-Phase Grid-Connected Converters with LCL Filter. *Journal of Power Electronics*, 11(4): 456-463.
- [6] Gajanayake CJ, Luo FL, Gooi HB, So PL, Siow LK. (2010). Extended-Boost Z-Source Inverters. *IEEE Transactions on Power Electronics*, 25(10): 2642-2652.
- [7] Adamowicz M, Strzelecki R, Vinnikov D. (2010). Cascaded Quasi-Z-Source Inverters for Renewable Energy Generation Systems. *Proceedings of Ecologic Vehicles and Renewable Energies Conference (EVER'10)*: 1-8.
- [8] Vinnikov D, Roasto I, Jalakas T, Strezelecki R, Adamowicz, MS. (2012). Analytical comparison of capacitor assisted and diode assisted cascaded quasi Z-source inverters. *Przegląd Elektrotechniczny*, 112(8):1392-1215.
- [9] Miaosen Shen, Jin Wang, Joseph A, Fang Zheng Peng, Tolbert LM, Adams DJ. (2006). Constant boost control of the Z-source inverter to minimize current ripple and voltage stress. *IEEE Transactions on Industry Applications*, 42(3):770-778.
- [10] Thangaprakash S, Krishnan A. (2010). Implementation and Critical Investigation on Modulation Schemes of Three Phase Impedance Source Inverter. *Iranian Journal of Electrical & Electronic Engineering*, 6(2):157-162.
- [11] Zong X, Gray PA, Lehn PW. (2016). New Metric Recommended for IEEE Standard 1547 to Limit Harmonics Injected Into Distorted Grids. *IEEE Transactions on Power Delivery*, 31(3):963-972.
- [12] Lal VN, Singh SN. (2017). Control and Performance Analysis of a Single-Stage Utility-Scale Grid-Connected PV System. *IEEE Systems Journal*, 11(3): 1601-1611.
- [13] Reddy D, Ramasamy S. (2017).A fuzzy logic MPPT controller based three phase grid-tied solar PV system with improved CPI voltage. Proceeding in Innovations in Power and Advanced Computing Technologies (i-PACT): 1-6.
- [14] Ellabban O, Van Mierlo J, Lataire A. (2012). A DSP-Based Dual-Loop Peak DC-link Voltage Control Strategy of the Z-Source Inverter. *IEEE Transactions on Power Electronics*, 27(9):4088-4097.

- [15] Vinnikov D, Roasto I, Jalakas T, Ott S.(2011). Extended Boost Quasi-Z-Source Inverters: Possibilities and Challenges. *Electronics And Electrical Engineering*, 112: 1392-1215.
- [16] Rostami H, Khaburi DA. (2009). Voltage gain comparison of different control methods of the Z-source inverter. *International of Electrical and Electronics Engineering*:268-272.
- [17] Delfino F, Denegri GB, Invernizzi M, Procopio R.(2010). A control algorithm for the maximum power point tracking and the reactive power injection from grid-connected PV systems. *IEEE Power and Energy Society General Meeting*.
- [18] Jain S, Agarwal V. (2007). Comparison of the performance of maximum power point tracking schemes applied to single-stage grid-connected photovoltaic systems. *IET Electric Power Application*, 1(55): 753-762.
- [19] Carli G, Singh A, Azeez NA, Williamson SS. (2018). Modelling, Design, Control, and Implementation of a Modified Z-Source Integrated PV/Grid/EV DC Charger/Inverter. *IEEE Transactions on Industrial Electronics*, 65(6): 5213-5220.
- [20] Altin N, Ozdemir S. (2013). Three-phase three-level grid interactive inverter with fuzzy logic based maximum power point tracking controller. *Journal of Energy Conversion and Management*, 69(6): 17-26.